

Correlations and Semi-Universal Relations Connecting Nuclear Matter and Neutron Stars

J. M. Lattimer

Department of Physics & Astronomy



60th International Winter Meeting on Nuclear Physics

Bormio, Italy, Jan. 22–26, 2024

Acknowledgements

Funding Support:

DOE - Nuclear Physics

DOE - Toward Exascale Astrophysics of Mergers and Supernovae (TEAMS)

NASA - Neutron Star Interior Composition ExploreR (NICER)

NSF - Neutrinos, Nuclear Astrophysics and Symmetries (PFC - N3AS)

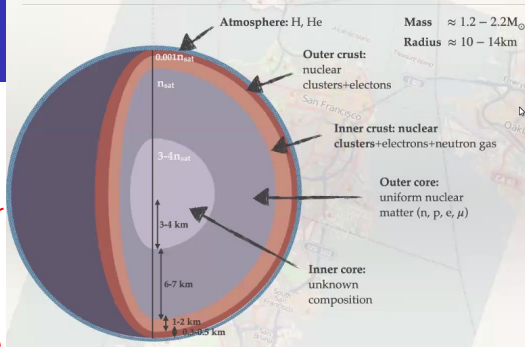
DOE - Nuclear Physics from Multi-Messenger Mergers (NP3M)

Recent Collaborators:

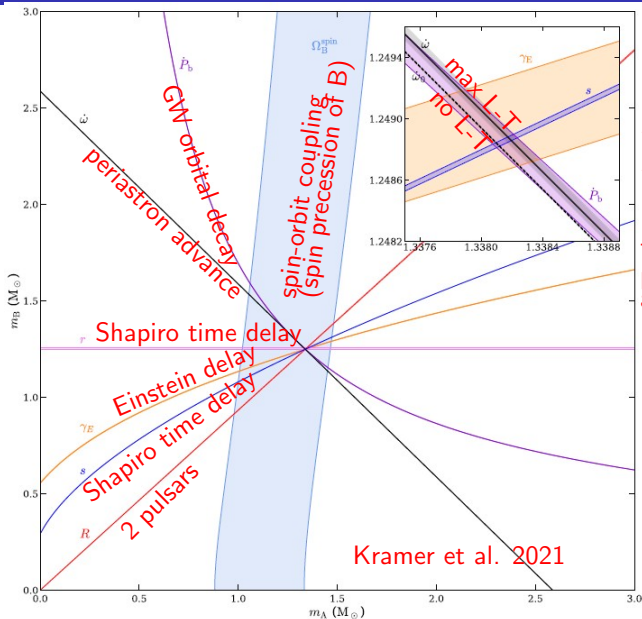
Boyang Sun (Stony Brook), Duncan Brown & Soumi De (Syracuse), Christian Drischler, Madappa Prakash & Tianqi Zhao (Ohio), Sophia Han (TDLI), Sanjay Reddy (INT), Achim Schwenk (Darmstadt), Andrew Steiner (Tennessee) & Ingo Tews (LANL)

Neutron Stars: Basics

- Nearly all known NSs are pulsars (rapidly rotating and highly magnetized) that emit X-ray, optical or radio beams from their poles, like a lighthouse.
- The radii of most NSs are about 12 km.
- Most, if not all, NSs are formed in the gravitational collapse of massive stars at the ends of their lives; some of those collapses produce black holes instead. Some massive NSs may be formed in the aftermath of a binary merger of two lower-massed neutron stars.
- The minimum possible NS mass is $0.1M_{\odot}$, but none are observed to be less massive than $1M_{\odot}$.



Pulsar Timing for PSR J0737-3039



$$m_A = 1.338185^{+12}_{-14} M_\odot$$

$$m_B = 1.248868^{+13}_{-11} M_\odot$$

These are the most precisely known masses of any astronomical objects.

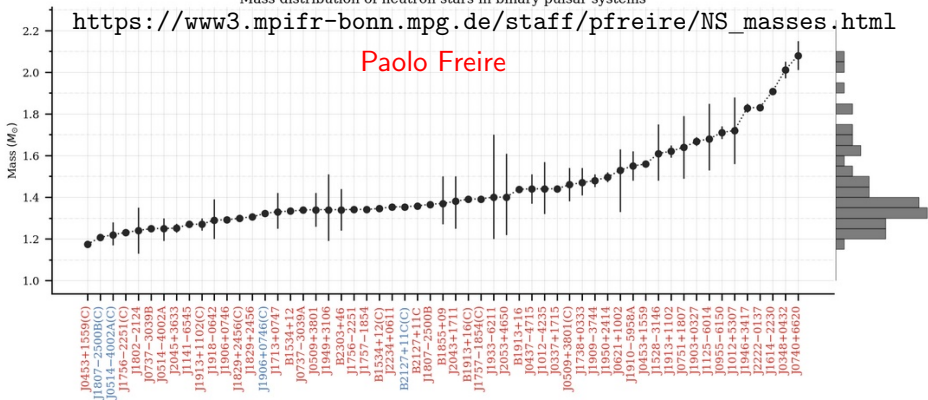
Kramer et al. 2021

Masses of Pulsars in Binaries from Pulsar Timing

Mass distribution of neutron stars in binary pulsar systems

https://www3.mpifr-bonn.mpg.de/staff/pfreire/NS_masses.html

Paolo Freire



Largest: $2.08 \pm 0.07 M_{\odot}$

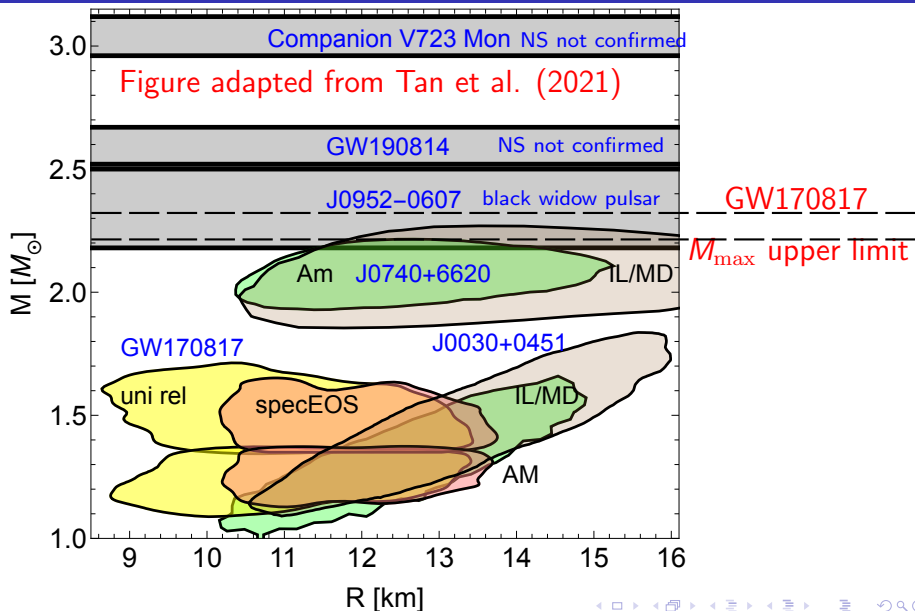
Smallest: $1.174 \pm 0.004 M_{\odot}$

Several other NS masses have been measured by other means, including some estimated to be more than $2M_{\odot}$ (e.g., black widow pulsars) and smaller than $1M_{\odot}$ (HESS J1731-347), but their mass uncertainties are generally large.

How Can a Neutron Star's Radius Be Measured?

- Flux = $\frac{\text{Luminosity}}{4\pi D^2} = \frac{4\pi R^2 \sigma_B T_s^4}{4\pi D^2} = \left(\frac{R}{D}\right)^2 \sigma_B T_s^4$
X-ray observations of quiescent neutron stars in low-mass X-ray binaries measure the flux and surface temperature T_s . Distance D somewhat uncertain; GR effects introduce an M dependence.
- $F_{Edd} = \frac{GMc}{\kappa D^2}$ X-ray observations of bursting neutron stars in accreting systems measure the Eddington flux F_{Edd} . κ is the poorly-known opacity; GR effects introduce an R dependence.
- X-ray phase-resolved spectroscopy of millisecond pulsars with nonuniform surface emissions (hot spots). NICER: PSR J0030+0451, PSR J0437-4715 (closest and brightest millisecond pulsar) and PSR J0740+6620 (most massive pulsar).
- $R_{1.4} = (11.5 \pm 0.3) \frac{\mathcal{M}}{M_\odot} \left(\frac{\tilde{\Lambda}}{800}\right)^{1/6} \text{ km}, \quad \mathcal{M} = \frac{(M_A M_B)^{3/5}}{(M_A + M_B)^{1/5}}$
GW observations of neutron star mergers measure the chirp mass \mathcal{M} and binary tidal deformability $\tilde{\Lambda}$ (GW170817).
- $I \propto M_A R_A^2$ Radio observations of extremely relativistic binary pulsars measure masses M_A, M_B and moment of inertia I_A from spin-orbit coupling [PSR J0737-3039 ($P_b = 0.102\text{d}$), PSR J1757-1854 (0.164 d), PSR J1946+2052 (0.078 d)].

Summary of Astrophysical Observations

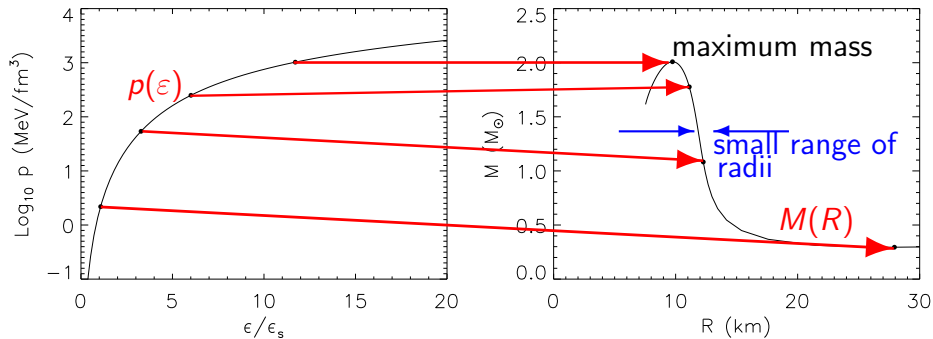


Neutron Star Structure

Tolman-Oppenheimer-Volkov equations

$$\frac{dp}{dr} = -\frac{G}{c^4} \frac{(mc^2 + 4\pi pr^3)(\epsilon + p)}{r(r - 2Gm/c^2)}$$

$$\frac{dm}{dr} = 4\pi \frac{\epsilon}{c^2} r^2$$

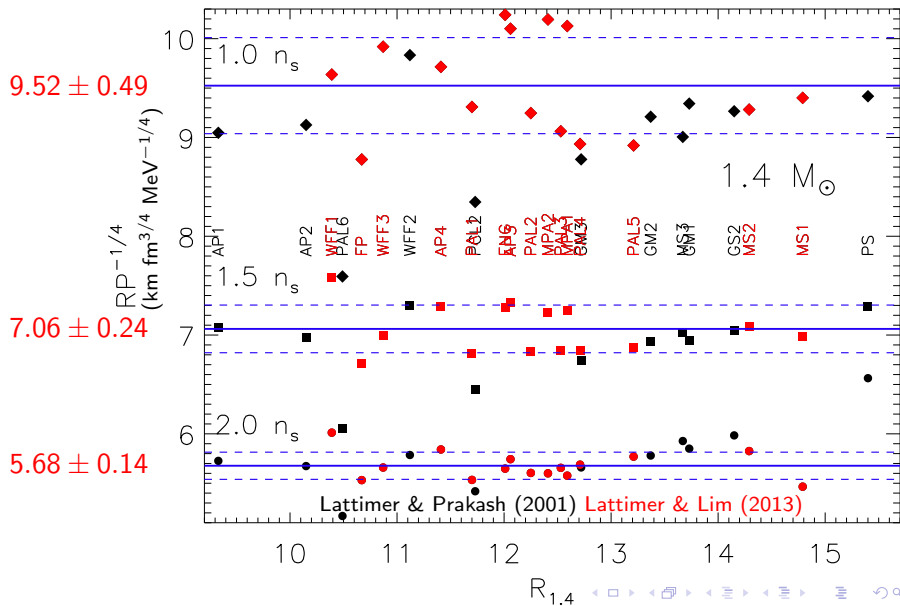


Equation of State

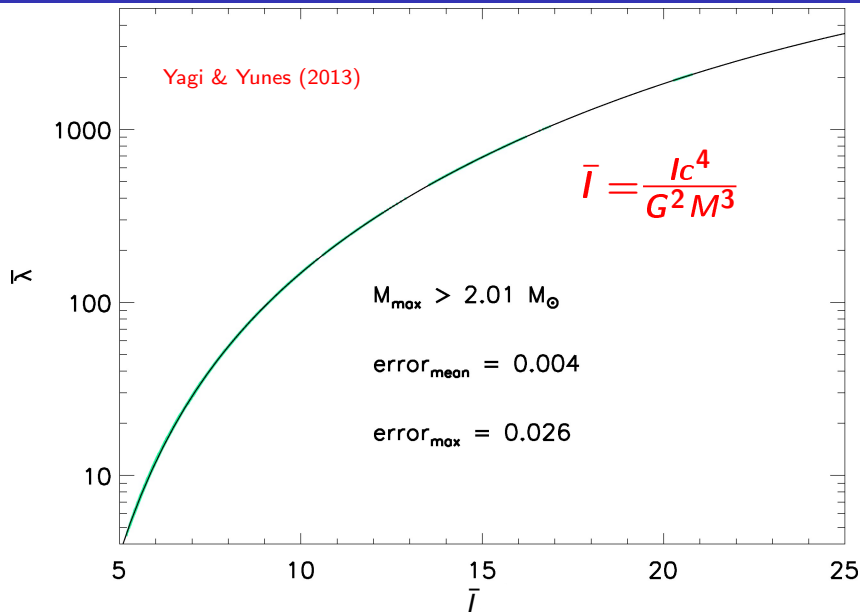


Observations

The Radius – Pressure Correlation



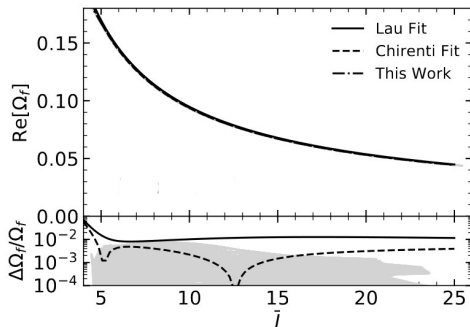
Tidal Deformatibility - Moment of Inertia



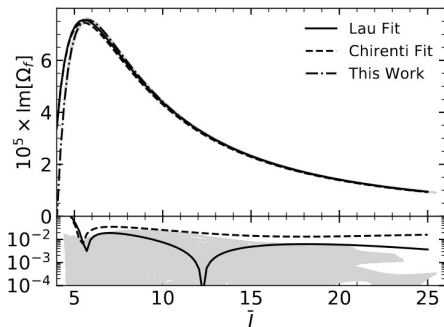
F-Mode Properties - Moment of Inertia

$$\Omega_f = \frac{GM\omega_f}{c^3}$$

Zhao & Lattimer 2022

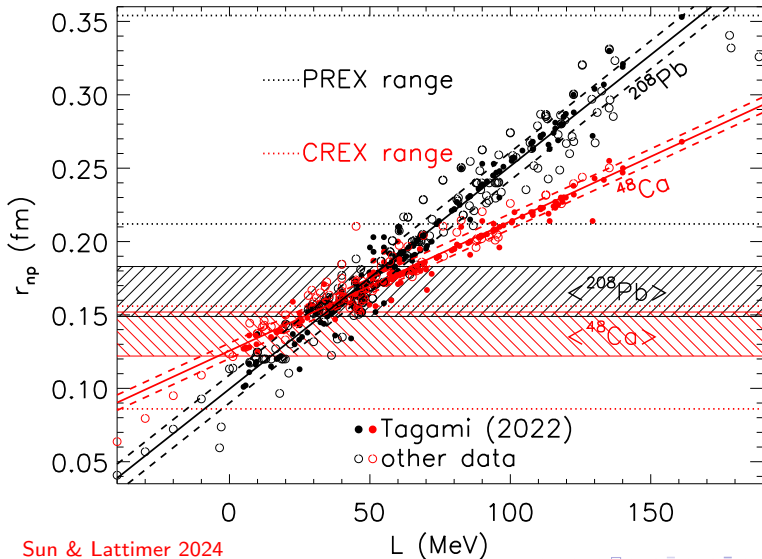


frequency



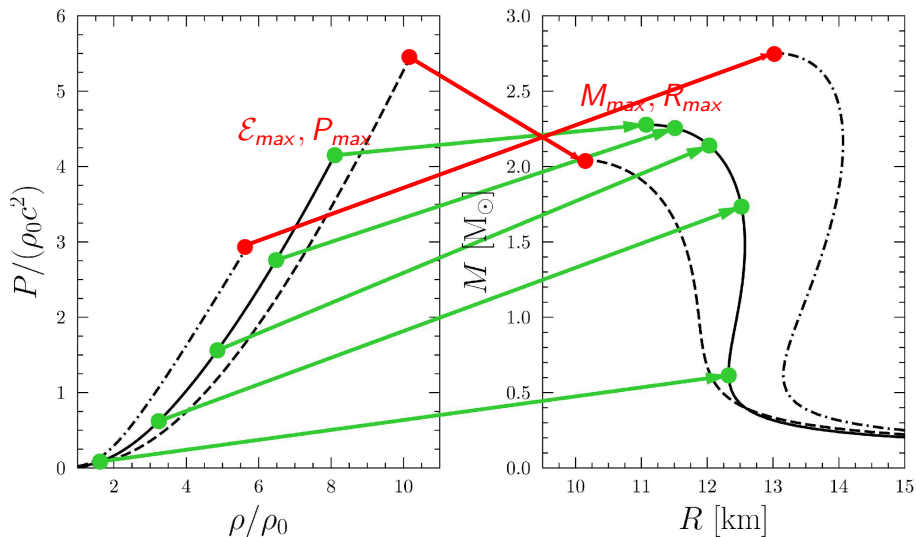
damping time

Neutron Skin Thickness - L

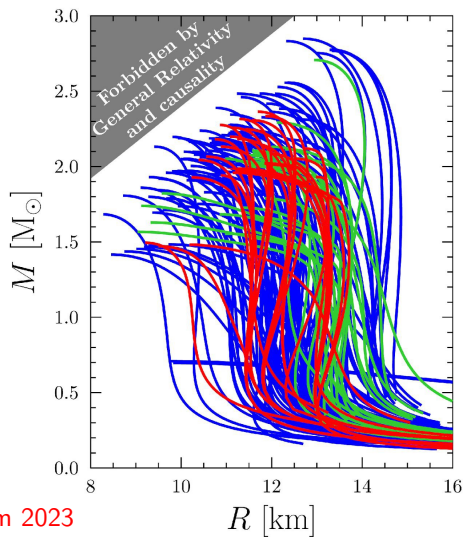
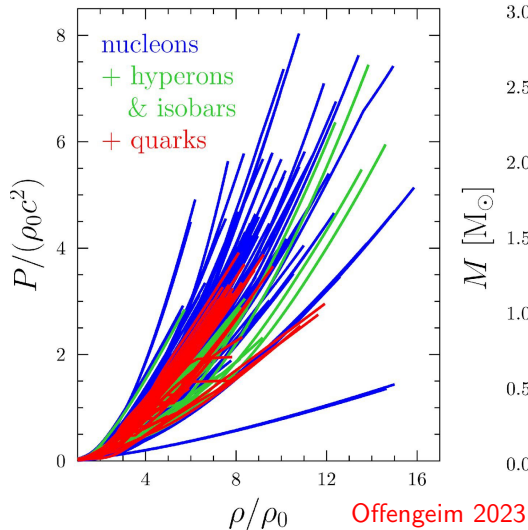


Sun & Lattimer 2024

Maximum Mass As a Unique Scaling Point



Varying the EOS



M_{\max} , R_{\max} , \mathcal{E}_{\max} , P_{\max} Correlations

- Ofengeim(2020) fitted \mathcal{E}_{\max} and P_{\max} with the functions

$$\mathcal{E}_{\max}, P_{\max} \simeq \left[\frac{a_{\mathcal{E},P}}{R_{\max} \cos \phi_{\mathcal{E},P} + (GM_{\max}/c^2) \sin \phi_{\mathcal{E},P} + d_{\mathcal{E},P}} \right]^{S_{\mathcal{E},P}}$$

with accuracies of about 3% and 8%, respectively.

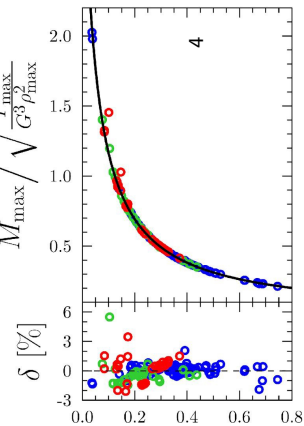
- Cai, Li and Zhang (2023) found a perturbative solution of the TOV equations in the parameter $x = P_c/\mathcal{E}_c$:

$$R \simeq \sqrt{\frac{3c^2}{2\pi G\mathcal{E}_c}} \left[\frac{x}{1+4x+3x^2} \right]^{1/2},$$
$$M \simeq \sqrt{\frac{54c^6}{\pi G^3\mathcal{E}_c}} \left[\frac{x}{1+4x+3x^2} \right]^{3/2}.$$

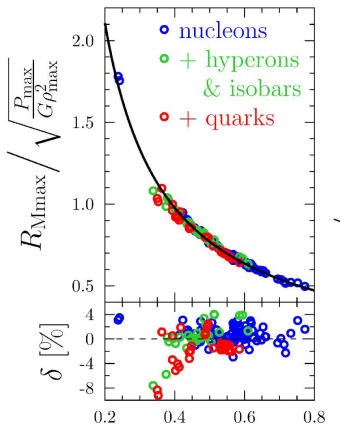
At M_{\max} , accuracies are 7% and 8%; at $1.4M_{\odot}$, they are 2% and 6%.

- Ofengeim et al. (2023) suggested fits for M_{\max} , R_{\max} :

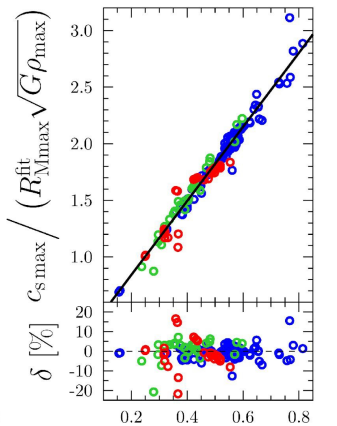
$$M_{\max} \simeq \frac{a_M \mathcal{E}_{\max}^{-1/2} x^{3/2}}{b_M + c_M x^{p_M} \mathcal{E}_{\max}^{q_M}}, \quad R_{\max} \simeq \frac{a_R \mathcal{E}_{\max}^{-1/2} x^{1/2}}{b_R + c_R x^{p_R} \mathcal{E}_{\max}^{q_R}}$$



$$\left(\frac{P_{\max}}{\rho_0 c^2}\right)^{1.41} \left(\frac{\rho_{\max}}{\rho_0}\right)^{-1.39}$$



$$\left(\frac{P_{\max}}{\rho_0 c^2}\right)^{0.52} \left(\frac{\rho_{\max}}{\rho_0}\right)^{-0.59}$$



$$\left(\frac{P_{\max}}{\rho_0 c^2}\right)^{0.76} \left(\frac{\rho_{\max}}{\rho_0}\right)^{-0.78}$$

M_{\max} , R_{\max} , \mathcal{E}_{\max} , P_{\max} Correlation

Ofengeim et al's finding suggest the power-law relations

$$\mathcal{E}_{c,\max} = (1.809 \pm 0.36) \left(\frac{R_{\max}}{10\text{km}} \right)^{-1.98} \left(\frac{M_{\max}}{M_{\odot}} \right)^{-0.171} \text{ GeV fm}^{-3},$$

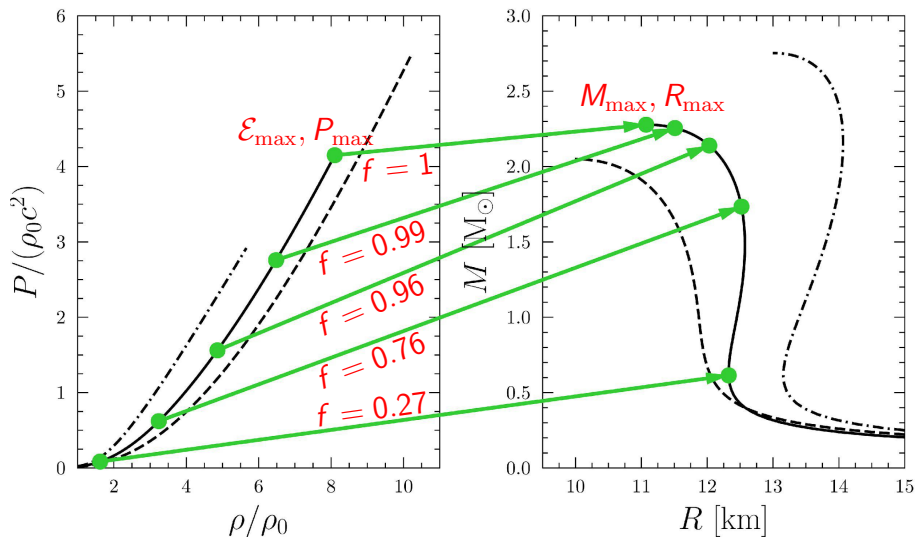
$$P_{c,\max} = (118.5 \pm 6.2) \left(\frac{R_{\max}}{10\text{km}} \right)^{-5.24} \left(\frac{M_{\max}}{M_{\odot}} \right)^{2.73} \text{ MeV fm}^{-3},$$

We find, in addition, that additional points along the $M - R$ curve, at $M = fM_{\max}$, have similarly accurate correlations:

$$\mathcal{E}_{c,f} = a_{\mathcal{E},f} \left(\frac{R_{fM_{\max}}}{10\text{km}} \right)^{b_{\mathcal{E},f}} \left(\frac{M_{\max}}{M_{\odot}} \right)^{c_{\mathcal{E},f}},$$

$$P_{c,f} = a_{P,f} \left(\frac{R_{fM_{\max}}}{10\text{km}} \right)^{b_{P,f}} \left(\frac{M_{\max}}{M_{\odot}} \right)^{c_{P,f}},$$

Correlations at $M = fM_{\max}$



Correlations with fM_{\max} and 2 R_f Values

$$\mathcal{E}_f = a_{\mathcal{E},f} \left(\frac{R_{f_1}}{10\text{km}} \right)^{b_{\mathcal{E},f_1}} \left(\frac{R_{f_2}}{10\text{km}} \right)^{c_{\mathcal{E},f_2}} \left(\frac{M_{\max}}{M_{\odot}} \right)^{d_{\mathcal{E},f}},$$

$$P_f = a_{P,f} \left(\frac{R_{f_1}}{10\text{km}} \right)^{b_{P,f_1}} \left(\frac{R_{f_2}}{10\text{km}} \right)^{c_{P,f_2}} \left(\frac{M_{\max}}{M_{\odot}} \right)^{d_{P,f}},$$

$f = M/M_{\max}$	$f_1 = M_1/M_{\max}$	$f_2 = M_2/M_{\max}$	$\Delta(\ln \mathcal{E}_f)$
1	1	1/2	0.0046
4/5	2/3	1/2	0.0036
2/3	2/3	3/5	0.0051
3/5	4/5	1/2	0.0025
1/2	2/3	1/2	0.0048
2/5	3/5	1/2	0.0047
$f = M/M_{\max}$	$f_1 = M_1/M_{\max}$	$f_2 = M_2/M_{\max}$	$\Delta(\ln P_f)$
1	1	1/2	0.019
4/5	4/5	1/2	0.0096
2/3	2/3	3/5	0.014
3/5	2/3	1/2	0.00069
1/2	3/5	1/2	0.020
2/5	3/5	1/2	0.032

greatly reduced uncertainties!

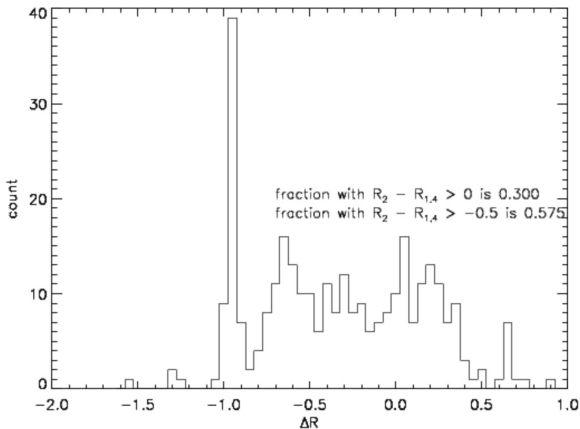
Importance of $\Delta R = R_{2.0} - R_{1.4}$

• J0030+0451:
 $R = 12.71^{+1.14}_{-1.19}$ km

• J0740+6620:
 $R = 12.39^{+1.30}_{-1.18}$ km

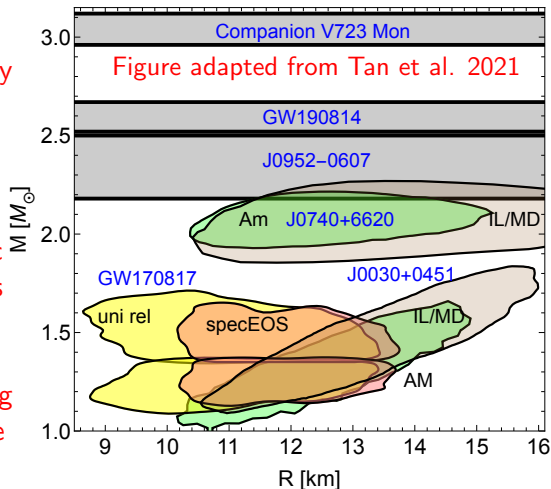
$\Delta R = -0.32^{+1.73}_{-1.68}$ km

313 Skyrme + RMF forces with $M_{max} \geq 2.0M_{\odot}$



Applications

- Analytic method of directly inverting TOV equations. Accuracies can be made arbitrarily high (number of R_f values). Existing techniques use parameterized EOS models in probabilistic (Bayesian) approaches having unquantified systematic uncertainties stemming from the model choice and parameter ranges (prior distributions).



- Correlations of $c_{s,\max}$ with M_{\max} and R_{\max} also exist (Ofengeim et al. 2023 found $\sim 10\%$ uncertainty), but accuracies are improved using power law-relations with $\geq 2 R_f$ values. Accurate values for specific f values would be useful for interpolating within the $\mathcal{E}_f - P_f$ grid. They could also allow probing the composition of the neutron star interior (phase transitions, etc.).
- Another unique feature of the $M - R$ diagram is the value of $(d^2M/dR^2)_{\max}$, which can be used in addition to M_{\max} and R_{\max} to improve accuracies.
- Correlations of $\tilde{\Lambda}$, \bar{I} and BE/M with M_{\max} and R_{\max} remain to be explored.